Microbial Pathogenesis 179 (2023) 106093

Contents lists available at ScienceDirect

Microbial Pathogenesis

journal homepage: www.elsevier.com/locate/micpath

Deciphering the antibiofilm potential of 2-Phenylethyl methyl ether (PEME), a bioactive compound of Kewda essential oil against *Staphylococcus aureus*

Priya Cheruvanachari [1], Subhaswaraj Pattnaik [1], Monika Mishra [1], Pratyush Pragyandipta, Animesh Pattnaik, Pradeep Kumar Naik [*]

Centre of Excellence in Natural Products and Therapeutics, Department of Biotechnology and Bioinformatics, Sambalpur University, Jyoti Vihar, Sambalpur, 768 019, Odisha, India

ARTICLE INFO

Keywords:
Biofilm
PEME
ESKAPE
Molecular docking
RT-PCR
Transcriptomics

ABSTRACT

Opportunistic pathogenic bacteria and their pathogenicity linked with biofilm infections become a severe issue as they resist the actions of multiple antimicrobial drugs. Naturally derived drugs having antibiofilm properties are more effective than chemically synthesized drugs. The plant derived essential oils are a rich source of phyto-constituents with widespread pharmacological values. In the present investigation, a major phytoconstituent, 2-Phenyl Ethyl Methyl Ether (PEME) of Kewda essential oil extracted from the flowers of *Pandanus odorifer* was explored for its prospective antimicrobial and anti-biofilm properties against ESKAPE pathogenic bacterial strains, *Staphylococcus aureus* and MTCC 740. The minimum inhibitory concentration (MIC) of PEME was found to be 50 mM against the tested bacterial strains. A gradual decrease in biofilm production was observed when PEME was treated with the sub-MIC concentration. The reduction in biofilm formation was noticeable from qualitative assay i.e., Congo Red Agar Assay (CRA) and further quantified by crystal violet staining assay. The decline in exopolysaccharides production was quantified, with the highest inhibition against MTCC 740 with a decrease of 71.76 ± 4.56% compared to untreated control. From the microscopic analysis (light and fluorescence microscopic method), PEME exhibited inhibitory effect on biofilm formation on the polystyrene surface. The *in silico* studies stated that PEME could invariably bind to biofilm associated target proteins. Further, transcriptomic data analysis suggested the role of PEME in the down-regulation of specific genes, *agrA*, *sarA*, *norA* and *mepR*, which are critically associated with bacterial virulence, biofilm dynamics and drug resistance patterns in *S. aureus*. Further, qRT-PCR analysis validated the role of PEME on biofilm inhibition by relative downregulation of *agrA*, *sarA*, *norA* and *mepR* genes. Further, advanced *in silico* methodologies could be employed in future investigations to validate its candidature as promising anti-biofilm agent.

1. Introduction

Biofilm is an extracellular polymeric matrix secreted by a group of microorganisms allowing them to be decisively attached to living or non-living surfaces. The attached biofilm matrix protects the encased microbial community from several environmental stress as it is tough for complete removal unless and until they are adequately treated [1]. The development of biofilm matrix over the biotic and abiotic surfaces becomes a significant concern and challenge to the public health sectors, medicine and pharma industries [2]. According to Wu et al. (2015), biofilm formation is considered an adaptation of microbes in response to an unfriendly environment [3]. Scientific data and analysis reports have clearly stated that the bacteria that are highly resistant to the antibiotics are more likely to be associated with the formation of recalcitrant biofilm matrices, and inhibition of biofilm formation with the help of antibiotics are nearly impossible. Bacteria such as *Staphylococcus*

Abbreviations: PEME, 2-Phenylethyl Methyl Ether; ESKAPE, Enterococcus faecium, Staphylococcus aureus, Klebsiella pneumoniae, Acinetobacter baumannii, Pseudomonas aeruginosa, Enterobacter spp.; RT-PCR, Reverse Transcriptase-Polymerase Chain Reaction.

* Corresponding author. Centre of Excellence in Natural Products and Therapeutics, Department of Biotechnology and Bioinformatics, Sambalpur University, Jyoti Vihar, Burla, Sambalpur, 768 019, Odisha, India.

E-mail addresses: pknaik1973@suniv.ac.in, pknaik1973@gmail.com (P.K. Naik).

[1] These authors contributed equally to this work.

https://doi.org/10.1016/j.micpath.2023.106093
Received 13 January 2023; Received in revised form 27 March 2023; Accepted 28 March 2023
Available online 31 March 2023

epidermidis, *S. aureus*, *Streptococcus* sp., *Pseudomonas aeruginosa* and *Enterococcus* sp. are often involved in biofilm-associated infections [4]. Specifically, the ESKAPE pathogens i.e., *Enterococcus faecium*, *Staphylococcus aureus*, *Klebsiella pneumoniae*, *Acinetobacter baumannii*, *Pseudomonas aeruginosa*, and *Enterobacter* spp., are resistant to a multitude of antibiotics owing to their ability to produce recalcitrant biofilms. These group of bacteria usually mutate their genes and get escape from the wrath of antimicrobial agents [5].

Due to the rapid emergence of multidrug-resistant microbes creating a selective pressure on the healthcare settings, there is a need to improve the existing antimicrobial agents or to develop alternative therapeutic agents. Keeping this problem in mind, medicinal plants with widespread pharmacological potential could be potential alternative agents to the current antibiotics to fight against microbial infections [6]. Medicinal plants owing to the presence of bioactive phytochemicals, reported to inhibit biofilm formation in pathogenic bacteria, including ESKAPE pathogens. Therefore, natural products are an essential source for discovering new antibacterial and anti-biofilm drugs [7,8]. Hence, plant-derived natural products including essential oils potentially challenge these deadly biofilm-forming pathogens [9]. The acceptance of natural products in therapeutics received widespread acceptance due to their traditional uses in folkloric medicines to cure several diseases [10]. Plant-derived essential oils are the rich source of bioactive phytocompounds such as monoterpenes and exhibited promising antibacterial and anti-biofilm activities against several drug resistant pathogens [11,12]. Similarly, *Pandanus odorifer* (Forssk.) Kuntze is an economically important aromatic plant and the characteristic aroma of the essential oil (known as Kewda oil) derived from male flower corresponds to the presence of bioactive 2-Phenyl ethyl methyl ether (PEME) and Terpinen-4-ol [13,14]. The essential oil from *P. odorifer* exhibited widespread folkloric uses to treat several diseases such as skin disorders, rheumatoid arthritis, and several forms of headache [13]. PEME is highly regarded as an essential component in several pharmaceutical industries, particularly as food additives and flavoring agents. Therefore, PEME has excellent potential to be developed as a substitute remedy for its promising therapeutic activities against recalcitrant biofilm-mediated infections. In the present study, the biofilm inhibitory activities of PEME against ESKAPE pathogen, *S. aureus* were determined, and the upregulation and downregulation of specific biofilms associated genes in *S. aureus* in response to PEME were validated through transcriptome and RT-PCR analysis.

2. Materials and methods

2.1. Chemicals and reagents

The chemicals such as Congo red, Crystal violet, acridine orange, *n*-Hexane, Luria-Bertani broth (LB), Mueller-Hinton Broth (MHB) were procured from HiMedia Pvt. Ltd., Mumbai, India. PEME was obtained from Sigma Aldrich, USA.

2.2. Processing of bacterial strains

The clinical strain, *S. aureus* was received from VIMSAR, Burla, Sambalpur, Odisha. The standard strain of *S. aureus* (MTCC 740) was purchased from IMTECH, Chandigarh, India. 0.5 McFarland standard was maintained for maintenance of bacterial culture in Luria–Bertani (LB) broth at 37 °C [14].

2.3. Evaluation of minimum inhibitory concentration (MIC)

The MIC of PEME against the test pathogens was determined as per the CLSI guidelines using the microdilution method. The microbial cultures were prepared in LB broth medium for 18 h and adjusted to 0.5 McFarland. The PEME was diluted in *n*-Hexane for stock concentration (100 mM). From the stock concentration (100 mM), serial dilutions of PEME (100, 50, 25, 12.5, 6.25, 3.125, 1.56, and 0.78 mM) were diluted in LB broth media with the addition of bacterial culture and incubated overnight at 37 °C. After the incubation period, the absorbance was taken at 600 nm. For blank, only LB broth media was taken, whereas, LB broth media and bacterial culture were taken as the negative control. The sub-MICs (i.e., ½ MIC) value was considered to evaluate antibiofilm activities [14–16].

2.4. Antibacterial activity of PEME

To study the antibacterial activity of PEME, an agar well diffusion assay using Kirby-Bauer method was performed. The sterile and solidified MH agar (MHA) plates were used to determine the antibacterial activity. Briefly, bacterial lawns were prepared by swabbing the overnight grown culture over the solidified agar medium. With the help of a sterile borer, 6 mm wells were prepared and both MIC and sub-MICs of PEME were added to the wells. *n*-Hexane was taken as control. The MH agar plates were incubated at 37 °C for 18–24 h. The hollow zone around the well was considered for antibacterial activity and the zone of inhibition (ZoI) was measured [17].

2.5. Inhibition of biofilm production by PEME

2.5.1. Biofilm formation assay (qualitative method)

For qualitative biofilm formation assay, Congo red agar (CRA) method was used to visualize the exopolysaccharide (EPS) formation on molten agar plates when the test pathogens were treated with sub-MIC of PEME as compared to untreated control [18]. CRA is composed of Brain Heart Infusion broth (37 mg/ml), Sucrose (50 mg/ml), agar agar (10 mg/ml) and Congo red (0.8 mg/ml). Briefly, the overnight-grown bacterial cultures treated with or without PEME were streaked onto the molten CRA plates and incubated overnight at 37 °C. The formation of black crystalline colonies corresponds to profuse EPS production (biofilm formation). In contrast, white colonies over the CRA plates correspond to inhibition of biofilm formation by a reduction in EPS production. In addition to CRA method, qualitative biofilm formation in test pathogens when treated with sub-MIC of PEME was determined by the test tube method to visualize the early recognition of the biofilm production by crystal violet staining. Briefly, the test tubes were inoculated with 0.5 McFarland bacterial culture in the presence of sub-MIC of PEME. After overnight incubation at 37 °C, the test tubes were washed with sterile PBS, followed by staining with crystal violet for 3–5 min. After excess removal of crystal violet stain, the presence or absence of major rings at the air-liquid interface and bottom surface of test tube designate the formation or inhibition of biofilm matrices.

2.5.2. Quantitative estimation of biofilm formation

Polystyrene-based 96-MTP was used to grow test microorganisms to form a biofilm matrix on the surface. The fresh bacterial cultures were inoculated into LB broth with or without sub-MIC of PEME and incubated overnight at 37 °C. After incubation, the broth was discarded, and the attached biofilm matrices were washed 2–3 times with sterile PBS for complete separation of cell debris. The attached biofilm matrices were then stained with 0.1% crystal violet (w/v) for 10 min, followed by the removal of excess stain. In the subsequent step, 95% ethanol was added to the wells, and spectrophotometric absorbance was measured at 540 nm [19].

$$\%\ \text{of biofilm inhibition} = \left[OD_{(control)} - OD_{(treated)} \ / \ OD_{(control)}\right] \text{ x } 100$$

2.5.3. Effect of PEME on biofilm formation using microscopic analysis

Sterile 24-MTP was used for microscopic examination. The fresh bacterial cultures were inoculated into the 24-MTP containing sterile coverslips dipped in LB broth medium loaded with sub-MIC of PEME. The 24-MTP was incubated overnight at 37 °C to allow biofilm formation over the surface of coverslips. The broth medium was discarded in

the subsequent step, and the coverslips were washed in sterile PBS. After the washing step, the biofilm matrix grown over the coverslips were visualised under the microscope. For light microscopic analysis, the attached biofilms on the coverslips were stained with 0.1% CV (w/v) for 20 min, followed by visual observation under a light microscope (Quasmo, PZRM-26, India) [14,20]. Like wise for the fluorescence microscopic analysis, the attached biofilm matrix were stained with 0.01% acridine orange (w/v) and incubated for 5–10 min under dark conditions, followed by observation under a fluorescence microscope (Nikon, eclipse TS2) [21]. Media with Bacterial culture were treated as untreated control.

2.6. In silico study

2.6.1. Protein preparation

The proteins responsible for biofilm formation and drug resistance in *S. aureus,* i.e., SarA (PDB ID:2FNP), Sortase A (PDB ID: 1T2P), AgrA (PDB ID: 4G4K), MepR (PDB ID: 3ECO) and Rot (PDB ID: 4Q77) were considered as target proteins for molecular docking. The obtained protein data Bank (PDB) structures were pre-processed, followed by the addition of hydrogen atoms using a protein preparation wizard (Schrödinger, Inc., NY). Prime side-chain prediction tool was used to identify the absent side-chain atoms of the amino acids, followed by repairing using Prime (Schrödinger, Inc., NY). Further, Macromodel (Schrodinger) and OPLS 2005 force field were employed for the energy minimization using Polak-Ribiere Conjugate Gradient (PRCG) algorithm [14,22].

2.6.2. Preparation of the ligand (PEME)

The molecular structure of PEME was prepared in ChemDraw and imported into Maestro (Schrödinger package) [22]. The ligand was also subjected to sequential energy minimization steps using PRCG algorithm. Eventually, several conformations of PEME were generated using the Ligprep module (Schrödinger package) [22,23].

2.6.3. Molecular docking of PEME to target proteins

A blind docking approach using SiteMap (Schrodinger package) was employed to determine the molecular interaction of PEME with selected target proteins [22]. After binding sites prediction, receptor grid boxes (dimension: 12 Å × 12 Å × 12 Å) were generated using Glide grid-receptor generation. In the subsequent step, the generated conformations of PEME were docked against all the forecasted binding site of target proteins through Glide XP (extra precision) algorithm (Schrodinger software package) and assessed their binding poses by the Glide XP_{Score} function [24,25].

2.7. Transcriptomic analysis

2.7.1. RNA extraction

The bacterial samples (untreated control and PEME treated) were processed using a HiMedia HiPurA extraction kit and eluted with 15 μl of RNase free water.

2.7.2. RNA integrity check

The RNA quality estimation was evaluated using RNA HS ScreenTape System (Catalog: 5067–5579, Agilent) in a 4150 TapeStation System (Catalog: G2992AA, Agilent) to calculate the RNA integrity number (RIN e), based on which the RNA quality was determined. About 2 μl of RNA sample was mixed with 1 μl of RNA ScreenTape Sample buffer and heat denatured at 72 °C for 3 min and immediately placed on ice for 2 min and loaded the sample on the Agilent 4150 TapeStation instrument. RIN e assigned by the software determines the integrity of RNA where RIN e values 1–5 are designated thorough degradation and 5–7 indicate partly degraded RNA, and RIN e value above 8 indicates good class of RNA.

2.7.3. RNA quantification

The concentration of RNA was evaluated on Qubit® 3.0 Fluorometer (Catalog: Q33216, ThermoFisher Scientific) using the QubitTM RNA HS Assay Kit with continuous fluorescence detection varying from 1 ng/μl to 100 ng/μl and two RNA standards. The dye followed by the buffer was diluted at a 1:200 ratio, and 1 μl of the RNA sample was thoroughly mixed with the dye mix and kept at room temperature for 2 min, and the interpretations were taken in the Qubit.3 Fluorometer. Before the measurement of the sample, the instrument was standardized using the two standards delivered in the kit.

2.7.4. Gene expression and transcriptomic analysis

2.7.4.1. Quality control check (QC) and pre-processing of the raw data. The evaluation of RNA-seq data starts with an analysis of raw reads, trimming of the adapter, read alignment, quantification of the gene and quality barrier after each analysis step. The QC of the raw reads was examined using FastQC (https://www.bioinformatics.babraham.ac.uk/projects/fastqc/, Babraham Bioinformatics, UK). The reads were trimmed using Cutadapt (v2.6) (Cutadapt removes adapter sequences from high-throughput sequencing reads to eliminate the adapter sequence and low-quality bases to invalidate the alignment biases [26].

2.7.4.2. Read alignment and quantification of raw data. The raw reads were mapped against the reference human genome using HISAT2 (v2.1.0) (HISAT: a fast spliced aligner with low memory requirements) to escape the loss of unannotated areas of the genome. The expression level of *S. aureus* and *S. aureus* treated with PEME transcripts was calculated according to the fragments per kilobase of exon per million mapped reads (FRKM) method by cufflinks (v2.2.1). The differential expression analysis and clean data were mapped back into the assembled transcriptome, and the read count for each gene was obtained from the mapping with cuffdiff (v2.2.1). Differential expression study of two samples was achieved using the cuffdiff. The p -value was modified using the q value. A q value < 0.05 and $|\log2 \text{ (fold change)}| \geq 0.8$ and ≤ -0.8 are set as the threshold for considerably differential expression [27,28].

2.7.4.3. Network analysis used for protein-protein interaction (PPI). Protein-protein interaction networks inspect the downstream association between proteins which is based on physical binding, genetic, functional connection, Gene Ontology (GO) and Kyoto Encyclopedia of Genes and Genomes (KEGG). The uniquely identified differentially expressed genes (DEGs) responsible for the antibiofilm activity of PEME were explored to determine the association between these DEGs with functionally related genes associated with bacterial infections, biofilm production, and drug resistance using STRING (https://string-db.org/). The taxonomy of the DEGs into the functional paths was directed through KEGG analysis (https://www.genome.jp/kegg/pathway.html).

2.8. Determination of relative gene expression using reverse transcription-polymerase chain reaction (RT-PCR) analysis

The effect of PEME on the relative expression levels of up-regulated and down-regulated DEGs was quantitatively validated by RT-PCR using the comparative cycle threshold ($2^{-\Delta\Delta CT}$) method [29]. Briefly, 2 μg of total RNA was used to synthesize cDNA which was further reverse-transcribed using PrimeScript™ RT reagent Kit. SYBR Green-based qPCR was performed on ABI ViiA 7 Real-Time PCR system (Applied Biosystems, Foster City, CA, USA). *rplD* was used as the endogenous control, and all the reactions were performed in triplicate. Relative gene expression was calculated using the comparative cycle threshold ($2^{-\Delta\Delta CT}$) method [29]. The details of the primers used in the present study for RT-PCR analysis were presented in Table S1 [30–34].

3. Results

3.1. Antibacterial and antibiofilm activity of PEME

The MIC value of PEME was observed to be 50 mM against both the clinical *S. aureus* and the MTCC 740 as shown in Fig. 1A. At the MIC level, PEME also exhibited moderate antibacterial activity with a zone of 10–12 mm against *S. aureus* and MTCC 740. (Fig. 1B). At sub-MIC level of PEME, a significant reduction in the production of EPS was observed over the molten CRA plates with characteristic white colonies as compared to dark black crystalline colonies in the untreated control (Fig. 2A). Similarly, the appearance of minor rings at the air-liquid interface and the bottom surface of test tubes when bacterial cultures were co-inoculated with sub-MIC level of PEME suggested the reduction in EPS production corresponding to inhibition of biofilm formation. As compared to treatment, in the untreated control, comparatively thicker major rings at the test tube surfaces were observed (Fig. 2B). PEME exhibited promising inhibitory effect on biofilm production in *S. aureus* and MTCC 740, with an inhibition of 59.32 ± 4.30 and 71.76 ± 4.56%, respectively at sub-MIC level (Fig. 3). The biofilm inhibitory effect of PEME was further confirmed by microscopic analysis. From both light and fluorescence microscopic analysis, a significant reduction in the biofilm production on the sterilized coverslips when treated with the sub-MIC of PEME was observed as evident from relatively lessed clustered biofilm matrices as compared to thick and clusterd biofilm matrices in the untreated control (Fig. 4).

3.2. Molecular docking study

A blind docking approach was used to dock the PEME with the selected proteins. In this approach, all the binding sites of the proteins were predicted using SiteMap (Table 1) and PEME was docked against each binding site. PEME exhibited the highest binding affinity towards SarA (a global regulatory protein) among the selected target proteins with a docking score of −4.023 kcal/mol and docking energy of −12.138 kcal/mol, followed by a docking score of −3.757 kcal/mol and docking energy of −18.129 kcal/mol with AgrA and a docking score of −3.559 kcal/mol and docking energy of −17.803 kcal/mol with MepR (a transcription regulator of multidrug efflux pump) (Table 1). The binding of PEME involved hydrogen bonding and hydrophobic interactions as shown in the ligplot (Figs. 5 and 6). It involved one hydrogen bond (dashed line) with the binding site amino acid Lys154(A) of 2FNP (SarA regulatory protein) (Fig. 5B), two hydrogen bonds with Asn31(A) and His35(A) of 3ECO (MepR regulatory protein) (Fig. 5C), and one hydrogen bond with Gln155(B) of 4G4K (AgrA regulatory protein) (Fig. 6A).

3.3. Transcriptomic analysis

3.3.1. Transcriptomic sequencing data analysis

Total 18.5 GB raw data of *Staphylococcus aureus* (G-Control_1 and G-Control_2) and *Staphylococcus aureus*/PEME (G-PEM_1 and G-PEM_2) were used to quality check and trimming for accuracy. The basic statistical parameters were passed the quality check. Table S2 shows the statistical summary of transcriptome-sequenced data. The *S. aureus* genome was used as a reference to support the reads by using the HISAT2 software. About 99.98% and 100.00% reads were plotted to the reference for the G-Control_1 and G-Control_2, whereas 100.00% reads were mapped to the reference for the G-PEME_1 and G-PEME_2,. The overall abstract of the mapping results was shown in Table S3. The cufflinks package was used to calculate the transcript abundances. The FPKM were estimated and the Cuffdiff package was used to find the difference at differentially expressed genes (DEGs). The p value was modified using the q value. A q value < 0.5 and log2 (fold change) > 0.8 (Up regulated gene) < -0.8 (Down regulated gene) was set as the threshold for significantly differential expression. Table S4 depicted the calculation of the number of DEGs observed.

3.3.2. PPI network analysis

From up-regulated (n = 9) DEGs, some selected genes used to construct PPI network, from which six are linked in different signal pathways, were assimilated using STRING website to survey the link between these DEGs. The gene *glms* and SAXN108_1366 showed interaction with each other. In contrast, from down-regulated (n = 16) DEGs, some selected genes were used to construct PPI network that are involved in the different signal pathways using STRING (https://string-db.org/) functional enrichment analysis to explore the connection between these DEGs (Fig. S1).

3.3.3. Functional annotations

Among the up-regulated DEGs, functional annotations of only five genes were available and depicted in Table 2. Similarly, among the sixteen down-regulated genes, only four such as *agrA*, *sarA*, *norA* and *mepR* are directly associated with the pathogenesis of *S. aureus* through quorum sensing interactions and biofilm formation. Hence, on treatment with PEME, the down regulation of above mentioned genes suggested the influence of PEME on the regulation of quorum sensing associated virulence and mitigation of biofilm formation (Table 3). Table 4 depicts the KEGG pathway analysis of up and down-regulated genes of *S. aureus* on treatment with PEME.

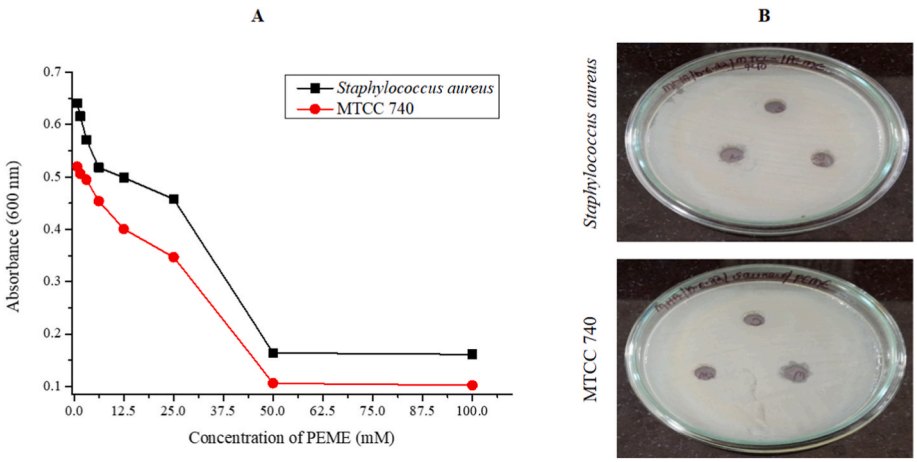

Fig. 1. (A) Determination of minimum inhibitory concentration (MIC) of PEME against clinical isolates of *Staphylococcus aureus* and reference strain MTCC 740, (B) Effect of PEME (at MIC level) on the growth of clinical bacterial isolates, *S. aureus* and reference strain, MTCC 740.

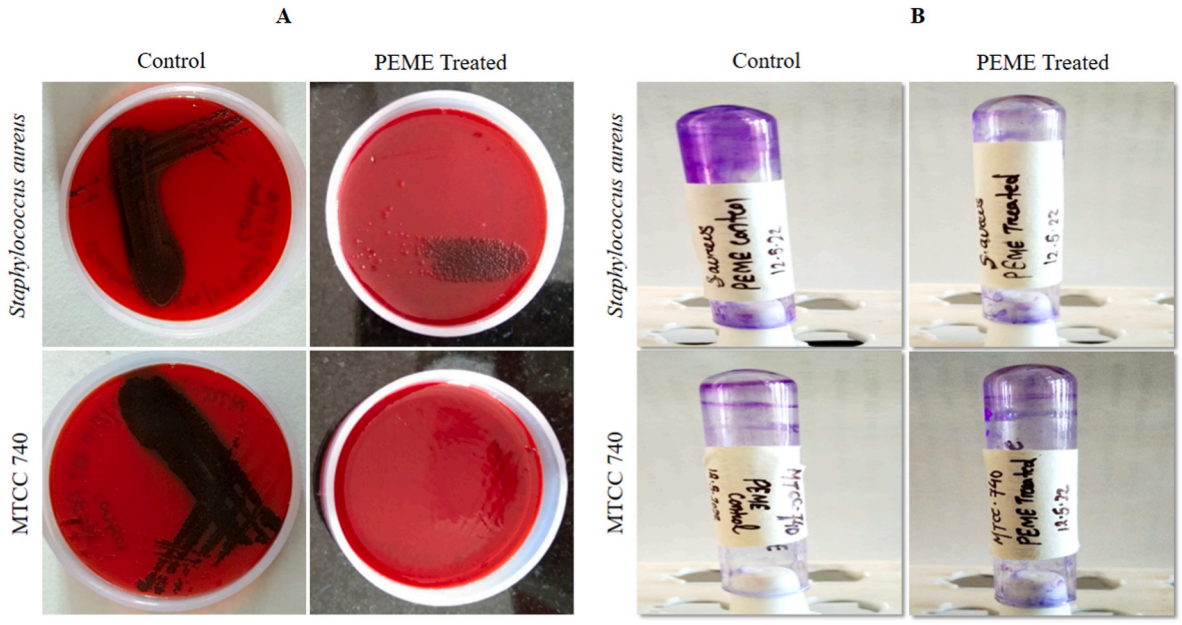

Fig. 2. Effect of sub-MICs of PEME on biofilm formation in clinical *Staphylococcus aureus* and its reference strains, MTCC 740 using (A) qualitative Congo red agar plate method and (B) qualitative crystal violet staining test tube method.

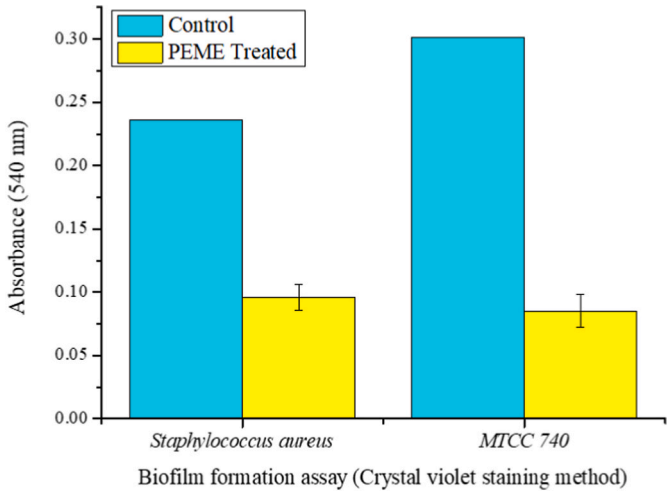

Fig. 3. Effect of sub-MIC of PEME on biofilm formation in clinical *Staphylococcus aureus* and its reference strain, MTCC 740 using quantitative biofilm formation assay (crystal violet staining method).

3.4. RT-PCR analysis

On treatment with sub-MIC of PEME, the biofilm associated genes in ESKAPE pathogen, *S. aureus* were relatively down regulated as compared to the normalized expression level of housekeeping gene, *rplD*. Fig. 7 depicted the relative down regulation of biofilm associated genes i.e. *agrA*, *sarA*, *norA*, and *mepR* (downregulated DEGs as per the transcriptome analysis) with 92.2, 91.4, 79.8, and 66.7% decrease in the expression levels respectively. Compared to the relative expression of downregulated DEGs, the relative expression of up-regulated DEGs (i.e. *glmS*, *saeS*, and *rpmC*) were comparatively higher with 96.8, 82.6, and 81.7% of expression levels, respectively when treated with sub-MIC of PEME as compared to the normalized expression of *rplD* (Fig. 7).

4. Discussion

PEME, an important aromatic volatile organic compound with widespread occurrence in plant-derived essential oils and microorganisms. PEME is considered as an important derivative of 2-Phenylethanol and contains widespread pharmaceutical relevance with special reference to cosmetics and food flavoring industries [35,36]. One of the most common use of PEME is its utilization in food industry as a flavoring agent and it can also be used as food additive for its peculiar aroma for the formulation of several beauty care products. It exhibited promising antibacterial and antifungal activities on several economically important pathogenic microorganisms. In the present study, moderate antibacterial activities at MIC concentration was shown by PEME against the test pathogens, *S. aureus* and MTCC 740. The results were in accordance with earlier reports depicting the antibacterial activities against several pathogens such as *S. aureus*, *E. faecalis*, *Escherichia coli*, *P. aeruginosa*, *K. pneumoniae* and *Salmonella* sp. [35]. In addition, the antifungal activities of PEME against fungal pathogens, *Candida albicans* and *Colletotrichum gloeosporioides* also suggested its widespread pharmacological potential [35,36]. Though, PEME has been reported for its antimicrobial properties, its inhibitory effect on biofilm mechanics in ESKAPE pathogens remin unexplored. Hence, in the present study, prospective biofilm inhibitory activities of PEME was evaluated. In our previous report, we have observed that Kewda essential oil exhibited promising inhibitory effect on biofilm formation against *S. aureus* and *K. pneumoniae*. As per the GC-MS report, PEME is the most abundant secondary metabolite present in the Kewda essential oil and could bbe instrumental in inferring the promising anti-biofilm activities. As both of the qualitative and quantitative biofilm assays provided a clear indication that, PEME strongly inhibited biofilm formation in *S. aureus* and reference strain, MTCC 740. Since the antibiofilm activity of PEME has not been reported, the present study is instrumental in developing PEME as a potential anti-biofilm agent in tackling the antimicrobial drug resistance phenomena in the near future.

From the molecular docking study, it was evident that PEME showed the highest binding affinity towards SarA (PDB ID: 2FNP) and AgrA (PDB ID: 4G4K) with a Glide XP score of −4.023 and −3.757 kcal/mol respectively. Since, the expression of *sarA* in *S. aureus* not only stabilizes the mRNA turn over but also critically affect the bacterial virulence properties by promoting survival in challenging environment; the favorable binding affinity of PEME towards SarA could eventually promote mitigation of biofilm production in *S. aureus* [37–39]. Similarly,

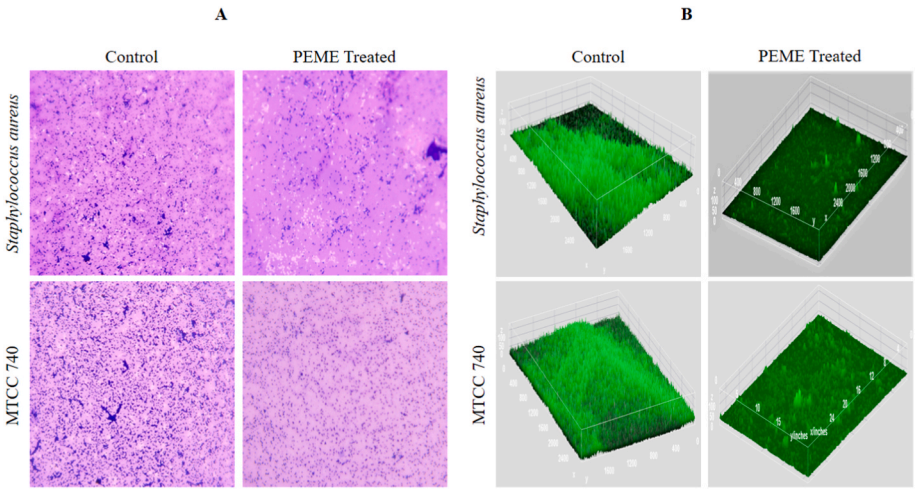

Fig. 4. Sub-MIC of PEME on biofilm formation in clinical *Staphylococcus aureus* and its reference strain, MTCC 740 using (A) Light microscopic analysis (crystal violet staining), and (B) Fluorescence microscopic analysis (acridine orange staining).

Table 1
Molecular docking results of 2-Phenylethyl methyl ether (PEME) with respect to different binding sites onto the proteins involved in pathogenesis, biofilm production and drug resistance of *Staphylococcus aureus*.

Site ID	Site score	Volume (Å)^3	Glide XP score (Kcal/mol)	Glide docking energy (Kcal/mol)
(a) PDB ID: 1T2P **(Sortase A, a surface associated protein)**				
1	1.023	482.2	−2.889	−18.857
2	0.959	415.4	−3.309	−19.783
3	1.049	342.6	−2.244	−21.089
4	0.875	220.5	−2.041	−15.240
5	0.786	116.3	−2.616	−16.980
6	0.790	110.8	−1.888	−15.487
7	0.651	105.6	**−3.342**	**−22.499**
8	0.688	92.27	−2.609	−20.189
(b) PDB ID: 2FNP **(SarA, a global regulatory protein)**				
1	0.941	142.7	−2.072	−18.339
2	0.853	148.2	−2.576	−18.839
3	0.780	128.3	−2.684	−19.25
4	0.648	75.12	−3.172	−15.202
5	0.727	162.6	1.219	−16.987
6	0.599	61.05	−2.290	−16.743
7	0.755	76.15	**−4.023**	**−12.138**
8	0.626	58.99	−2.175	−15.914
(c) PDB ID: 3ECO **(MepR, a transcriptional regulator of multidrug efflux pump)**				
1	0.944	262.7	**−3.559**	**−17.803**
2	0.977	248.3	−3.441	−17.008
(d) PDB ID: 4G4K **(AgrA, a transcriptional regulator)**				
1	1.027	531.6	**−3.757**	**−18.129**
2	0.609	78.55	−2.254	−16.783
(e) PDB ID: 4Q77 **(Rot, a global regulator of virulence genes)**				
1	0.663	130.7	**−2.526**	**−17.633**
2	0.530	45.62	−1.940	−18.192
3	0.574	101.5	−1.149	−21.606

the binding potential of PEME towards transcriptional regulatory protein, AgrA, an important component of the Two-component systems (TCSs) could eventually affect the bacterial virulence profile and regulation of several secreted proteins of pathophysiological importance [39,40]. Since, the selected target proteins of interests are accountable for inferring bacterial infections, host defence mechanisms and biofilm dynamics, the suitable interaction of PEME with these proteins could recommend its application as a promising therapeutic agent against biofilm mediated *S. aureus* infections. Further, *in silico* studies could be taken into consideration in the future course of time with positive control to assess the suitability of PEME as potential mitigator of biofilm-mediated chronic infections.

Since, mRNA sequencing analysis for transcriptome profiling critically provide an overview of all the transcripts, transcriptomic analysis of mRNA isolated from PEME treated *S. aureus* (*S. aureus*/PEME) was performed [41]. The mRNA sequencing analysis revealed that, on treatment with PEME, the up-regulated genes were generally associated with fatty acid metabolism, cellular metabolic processes, amino acid biosynthesis etc. which were in accordance to earlier report depicting the upregulation of histidine metabolism and lysisne biosynthesis processes in *S. aureus* when treated with *Litsea cubeba* L. essential oil [42]. As per the transcriptome profiling reports, several genes (e.g. *agrA*, *norA*, *mepR*, *sarA*) of interests which are directly or indirectly associated with two component signalling systems, bacterial virulence, biofilm formation and drug resistance patterns were considered as DEGs which were down regulated [43,44]. From the KEGG pathway enrichment analysis, it has been observed that the up regulated DEGs were linked to pathways associated with amino acid metabolism, nucleotide biosynthesis etc. Meanwhile, the down regulated DEGs were linked to amino acid biosynthesis, two component signalling systems and quorum sensing. The KEGG pathway enrichment analysis results were in accordance to earlier report where similar observations were reported [42]. Since the TCSs and fatty acid metabolism pathways are associated biofilm formation as observed from KEGG pathway enrichment analysis, PEME could be considered as promising inhibitory agent against recalcitrant biofilm dyanmics in drug resistant *S. aureus* [45].

The transcriptomic results were further validated through RT-PCR analysis by quantification of the relative expression of both up-regulated and down-regulated DEGs as compared to the normalized expression level of housekeeping gene, *rplD*. As evident from relative gene expression level studies, the biofilm associated genes i.e. *agrA*, *sarA*, *mepR*, and *norA* were significantly downregulated on treatment with sub-MIC of PEME. The relatively higher decrease in the expression level of *agrA* and *sarA* genes, when treated with PEME was in accordance with the earlier report depicting the inhibitory effect of baicalein, a potent bioactive compound from *Scutellaria baicalensis* [30]. The significant decrease in the levels of *agrA* and *sarA* genes suggested the role of PEME in mitigation of biofilm related infections caused by *S. aureus*. Similarly, the decreased expression of *norA* and *mepR* suggested the role of PEME on the efflux mediated response in test pathogen thereby promoting the antibiotic penetrance into the bacterial system. The results were in accordance to earlier report, where the bioactive compound from *Garcinia mangostana*, Alpha mangostin significantly altered the relative expression levels of genes associated with biofilm formation, efflum machinery and persister cell formation [29]. Hence, from the transcriptomic analysis followed by studies on relative gene expression levels, PEME could be considered as potent therapeutic agent against

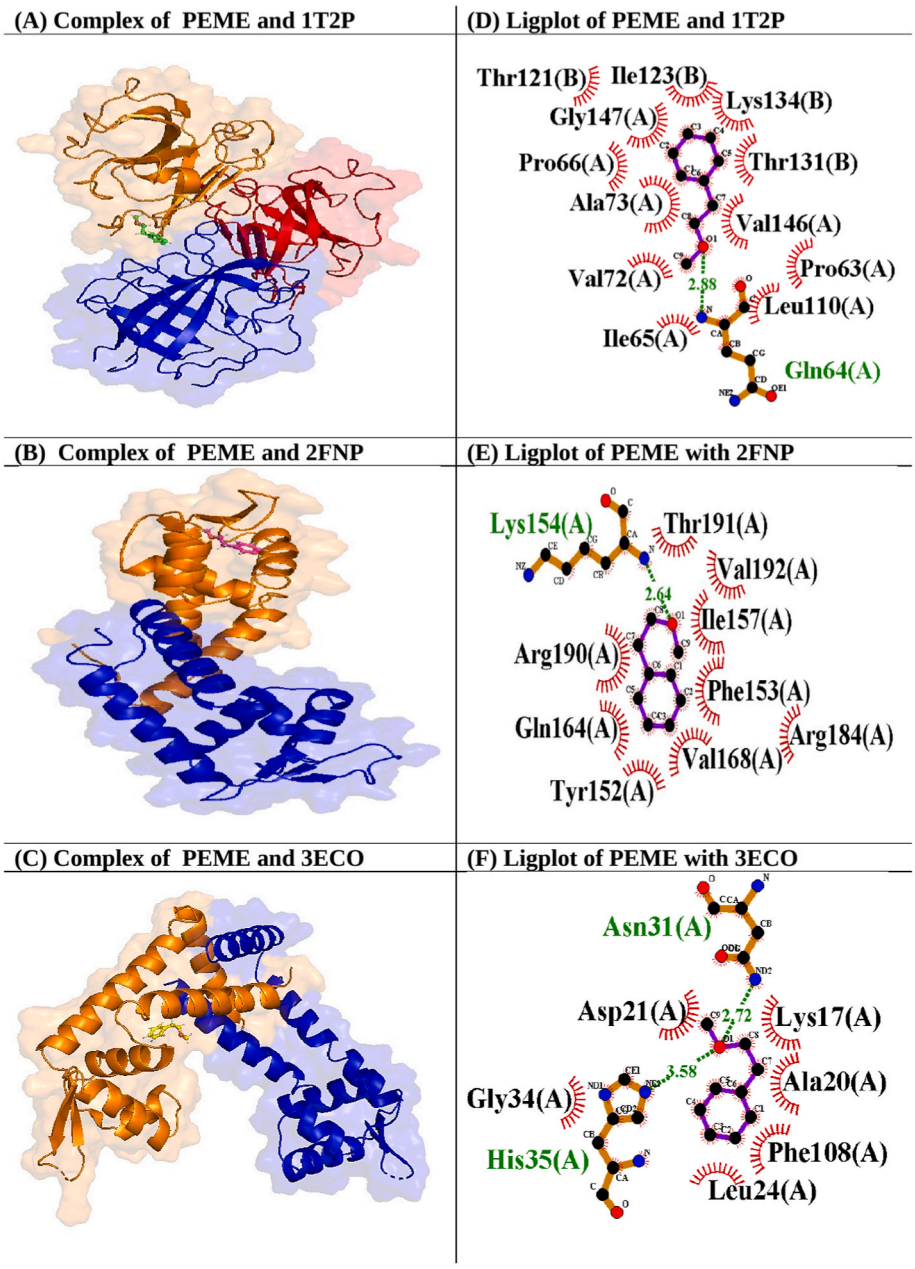

Fig. 5. Molecular docking of PEME onto the proteins involve in pathogenesis, biofilm production and drug resistance of *S. aureus*. PEME is well accommodated inside the binding site of (A) 1T2P, (B) 2FNP and (C) 3ECO. The ligplot analysis of PEME showing the interactions with binding site amino acids of (D) 1T2P, (E) 2FNP and (F) 3ECO. Its binding involved both hydrogen bonds represented as dotted (green) lines and hydrophobic interactions denoted with curved (red) lines.

biofilm mediated infections and drug resistance in *S. aureus*. Similarly, the relatively higher expression levels of upregulated DEGs as compared to downregulated DEGs suggested their possible impact on bacterial metabolism and stress response mechanism. However, further confirmative analysis could be incorporated to decipher its role as promising anti-biofilm agent using advanced in silico tools for predictions of its binding stability towards target proteins of interest and probable drug likeness and toxicity profile. The results suggested that these genes could be specifically targeted against antimicrobial resistance shown by *S. aureus* and PEME could be a lead molecule in this regard. Thus, PEME could be considered for its possible role in managing the biofilm-linked infections in the near future.

5. Conclusion

From the present study, it was observed that PEME showed moderate antibacterial properties and exhibited promising biofilm inhibitory properties against the test pathogen, *S. aureus*. The biofilm inhibition potential of PEME could be attributed to the down regulation of specific genes (i.e. *sarA*, *agrA*, *norA* and *mepR*), which are directly associated with bacterial pathogenesis and biofilm mediated infections as evident from the transcriptomic profiling of mRNA. The quantitative down-regulation of these biofilm associated genes in response to PEME treatment further validated its candidature as promising anti-biofilm agent. Further, *in silico* studies to evaluate the interaction of PEME towards the selected target proteins of interest also inferred the role of PEME in down regulation of these proteins. This hypothesis could be further validated through molecular dynamics simulation (MDS) and comparison with a positive control in the future course of work to ascertain its role in mitigation of biofilm and drug resistance patterns in pathogenic microorganisms. In addition, PEME could be used in combination with other suitable drugs to determine the synergistic role in biofilm

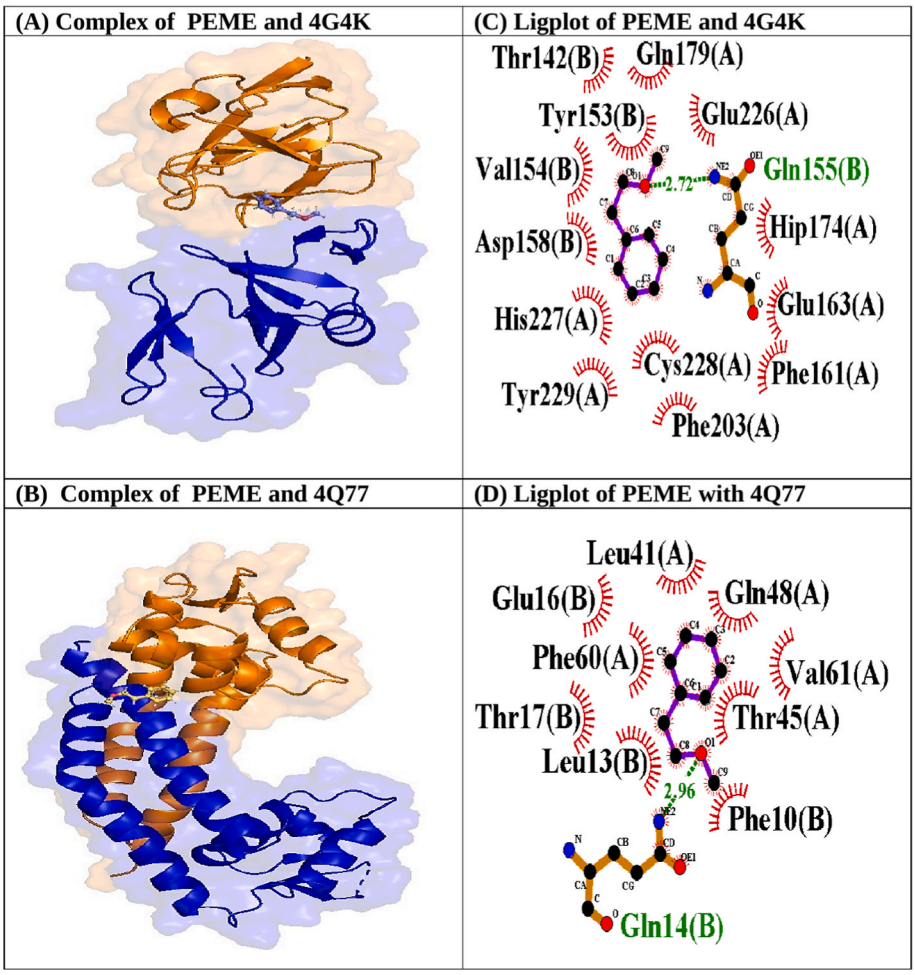

Fig. 6. Molecular docking of PEME onto the proteins involve in pathogenesis, biofilm production and drug resistance of *S. aureus*. PEME is well accommodated inside the binding site of (A) 4G4K and (B) 4Q77. The ligplot analysis of PEME showing the interactions with binding site amino acids of (C) 4G4K and (D) 4Q77. Its binding involved both hydrogen bonds represented as dotted (green) lines and hydrophobic interactions denoted with curved (red) lines.

Table 2
Transcriptomic analysis of up-regulated gens of *Staphylococcus aureus* on treatment with 2-Phenylethyl methyl ether (PEME).

Sl. No.	Gene	Biological process	GOTerm ID	Molecular function	GOTerm ID	Cellular component	GOTerm ID
1.	AID39897.1	Pathogenesis	GO:0009405	Nucleic acid binding	GO:0003676	Integral component of membrane	GO:0016021
				Catalytic activity	GO:0003824		
		Interspecies interaction between organisms	GO:0044419	Endonuclease activity	GO:0004519	Cell periphery	GO:0071944
				Hydrolase activity	GO:0016787	Cellular anatomical entity	GO:0110165
2.	SAXN108_1366	Metabolic process	GO:0006082	Nucleic acid binding	GO:0003676	Intracellular	GO:0005622
		Fatty acid metabolism,	GO:0006631	Catalytic activity	GO:0003824	Cytoplasm	GO:0005737
		Carboxylic acid metabolic process	GO:0019752	Lyase activity	GO:0016829	Cytosol	GO:0005829
		Cellular respiration	GO:0045333	Hydrolyase activity	GO:0016836	Cellular anatomical entity	GO:0110165
3.	*glmS*	Metabolic process	GO:0008152	Catalytic activity	GO:0003824	Intracellular	GO:0005622
		Biosynthetic process	GO:0009058	Transferase activity	GO:0016740	cytoplasm	GO:0005737
		Nitrogen compound metabolic process	GO:0006807				
		Carboxylic acid metabolic process	GO:0019752			Cellular anatomical entity	GO:0110165
		Cellular process	GO:0009987				
4.	*rpmC*	Metabolic process	GO:0008152	Structural constituent of ribosome	GO:0003735	Intracellular	GO:0005622
		Biosynthetic process	GO:0009058			Cytoplasm	GO:0005737
		Gene expression	GO:0010467	Structural molecule activity	GO:0005198	Cellular anatomical entity	GO:0110165
		Translation	GO:0006412			Large ribosomal subunit	GO:0015934
5.	*saeS*	Phosphorelay signal transduction system	GO:0000160	Protein kinase activity	GO:0004672	Integral component of membrane	GO:0016021
		Protein phosphorylation	GO:0006468	Transferase activity	GO:0016740	Cell periphery	GO:0071944
		Signal transduction	GO:0007165				
		Pathogenesis	GO:0009405	Phosphorelay sensor kinase activity	GO:0000155	Cellular anatomical entity	GO:0110165
		Intracellular signal transduction	GO:0035556				

Table 3
Transcriptomic analysis of down-regulated genes of *Staphylococcus aureus* on treatment with 2-Phenylethyl methyl ether (PEME).

Sl. No.	Gene	Biological process	GOTerm ID	Molecular function	GOTerm ID	Cellular component	GOTerm ID
1.	*agrA* (SAXN108_2132)	Phosphorelay signal transduction system	GO:0000160	Nucleic acid binding	GO:0003676	Intracellular	GO:0005622
		Cell communication	GO:0007154				
		Signal transduction	GO:0007165	Binding	GO:0005488	Cytoplasm	GO:0005737
		Cellular process	GO:0009987				
		Signaling	GO:0023052	Organic cyclic compound binding	GO:0097159	Cellular anatomical entity	GO:0110165
		Intracellular signal transduction	GO:0035556				
2.	*mepR* (AID38823.1)	Regulation of transcription, DNA-templated	GO:0006355	Nucleic acid binding	GO:0003676	Intracellular	GO:0005622
		Regulation of gene expression	GO:0010468				
		Regulation of metabolic process	GO:0019222	Organic cyclic compound binding	GO:0097159	Cytoplasm	GO:0005737
		Regulation of biological process	GO:0050789				
		Regulation of cellular process	GO:0050794	Transcription regulator activity	GO:0140110	Cellular anatomical entity	GO:0110165
		Biological regulation	GO:0065007				
3.	SAXN108_0407	Metabolic process	GO:0008152	Binding	GO:0005488	Intracellular	GO:0005622
		Cellular process	GO:0009987	Transferase activity	GO:0016740	Cytoplasm	GO:0005737
		Cellular metabolic process	GO:0044237	Catalytic activity	GO:0003824	Cellular anatomical entity	GO:0110165
4.	*norA* (SAXN108_0763)	Transport	GO:0006810	Transporter activity	GO:0005215	Plasma membrane	GO:0005886
		Cellular process	GO:0009987			Integral component of membrane	GO:0016021
		Response to antibiotic	GO:0046677	Transmembrane transporter activity	GO:0022857	Cell periphery	GO:0071944
		Transmembrane transport	GO:0055085			Cellular anatomical entity	GO:0110165
5.	SAXN108_1143	Metabolic process	GO:0008152	Catalytic activity	GO:0003824	Plasma membrane	GO:0005886
		Cellular process	GO:0009987	Binding	GO:0005488	Membrane	GO:0016020
		Cellular metabolic process	GO:0044237	Electron transfer activity	GO:0009055	Cell periphery	GO:0071944
		Cellular respiration	GO:0045333	Organic cyclic compound binding	GO:0097159	Cellular anatomical entity	GO:0110165
6.	SAXN108_1534	Metabolic process	GO:0008152	Catalytic activity	GO:0003824	Intracellular	GO:0005622
		Cellular process	GO:0009987	Binding	GO:0005488	Cytoplasm	GO:0005737
		Cellular metabolic process	GO:0044237	Organic cyclic compound binding	GO:0097159	Cytosol	GO:0005829
		Primary metabolic process	GO:0044238	Oxidoreductase activity	GO:0016491	Cellular anatomical entity	GO:0110165
7.	*metE* (SAXN108_0406)	Metabolic process	GO:0008152	Catalytic activity	GO:0003824	Intracellular	GO:0005622
		Cellular process	GO:0009987	Binding	GO:0005488	Cytoplasm	GO:0005737
		Cellular metabolic process	GO:0044237	Transferase activity	GO:0016740	Cytosol	GO:0005829
		Small molecule biosynthetic process	GO:0044283	Metal ion binding	GO:0046872	Cellular anatomical entity	GO:0110165
8.	*rplA* (SAXN108_0592)	Metabolic process	GO:0008152	Nucleic acid binding	GO:0003676	Intracellular	GO:0005622
		Cellular process	GO:0009987	Structural constituent of ribosome	GO:0003735	Cytoplasm	GO:0005737
		Cellular metabolic process	GO:0044237	Organic cyclic compound binding	GO:0097159	Cytosol	GO:0005829
		Biological regulation	GO:0065007	Heterocyclic compound binding	GO:1901363	Cellular anatomical entity	GO:0110165
9.	*rplB* (SAXN108_2496)	Metabolic process	GO:0008152	Nucleic acid binding	GO:0003676	Intracellular	GO:0005622
		Cellular process	GO:0009987	Catalytic activity	GO:0003824	Cytoplasm	GO:0005737
		Cellular metabolic process	GO:0044237	Transferase activity	GO:0016740	Cytosol	GO:0005829
		Gene expression	GO:0010467	Heterocyclic compound binding	GO:1901363	Cellular anatomical entity	GO:0110165
10.	*rplK* (SAXN108_0591)	Metabolic process	GO:0008152	Nucleic acid binding	GO:0003676	Intracellular	GO:0005622
		Cellular process	GO:0009987	Binding	GO:0005488	Cytoplasm	GO:0005737
		Cellular metabolic process	GO:0044237	Heterocyclic compound binding	GO:1901363	Cytosol	GO:0005829
		Cellular component biogenesis	GO:0044085	Organic cyclic compound binding	GO:0097159	Cellular anatomical entity	GO:0110165
11.	*sarA* (SAXN108_0683)	Pathogenesis	GO:0009405	Nucleic acid binding	GO:0003676	Intracellular	GO:0005622
		Regulation of biosynthetic process	GO:0009889	Binding	GO:0005488	Cytoplasm	GO:0005737
		Regulation of gene expression	GO:0010468	Heterocyclic compound binding	GO:1901363		
		Interspecies interaction between organisms	GO:0044419	Organic cyclic compound binding	GO:0097159	Cellular anatomical entity	GO:0110165

inhibition in ESKAPE pathogens.

Funding

This work was supported by the Department of Biotechnology, Govt. of India (File No. BT/INF/22/SP45357/2022I) under DBT BUILDER; and Science and Engineering Research Board (SERB), Department of Science and Technology, Govt. of India for the award of National Post-Doctoral Fellowship (N-PDF) [grant number: PDF/2021/001260].

Table 4
KEGG pathways enrichment analysis of up and down-regulated genes of *Staphylococcus aureus* on treatment with 2-Phenylethyl methyl ether (PEME).

UP-REGULATED GENES			DOWN_REGULATED GENES		
Gene name	KEGG_ID	Pathways	Gene name	KEGG_ID	Pathways
glmS	sae01250	Biosynthesis of nucleotide sugars	*metE*	sae01100	Metabolic pathways
	sae00250	Alanine, aspartate and glutamate metabolism		sae01230	Biosynthesis of amino acids
	sae00520	Amino sugar and nucleotide sugar metabolism		sae00270	Cysteine and methionine metabolism
	sae01100	Metabolic pathways		sae00450	Selenocompound metabolism
rpmC	sae03010	NWMN_2150 (rplW) NWMN_2141 (rplX) NWMN_2144 (rpmC) NWMN_2134 (rpmD) NWMN_2151 (rplD) NWMN_0014		sae01110	Biosynthesis of secondary metabolites
saeS	sae02020	Two-component system	*rplB/ rpsM*	sae03010	Ribosome
			agrA	sae00261	Monobactam biosynthesis
				sae01210	2-Oxocarboxylic acid metabolism
				sae01220	Degradation of aromatic compounds
				sae02024	Quorum sensing
				sae02020	Two-component system
			norA	sae01110	Biosynthesis of secondary metabolites
				sae02020	Two-component system
				sae00350	Tyrosine metabolism
				sae02024	Quorum sensing
				sae01100	Metabolic pathways

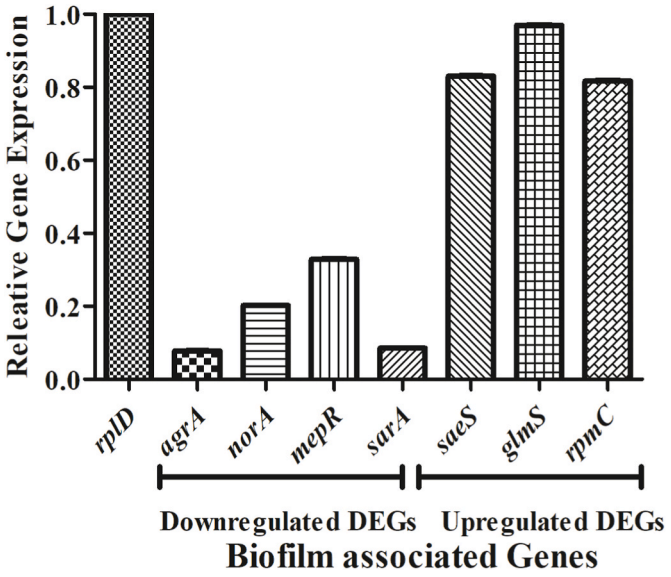

Fig. 7. Effect of sub-MIC of PEME on the relative expression levels of upregulated DEGs (*saeS*, *glmS*, and *rpmC*) and downregulated DEGs (*agrA*, *sarA*, *norA*, and *mepR*) as compared to normalized expression level of housekeeping gene, *rplD*.

Conflict of interest

No conflict of interests as declared by the authors.

CRediT authorship contribution statement

Priya Cheruvanachari: Writing – original draft, Resources, Project administration, Methodology, Investigation, Formal analysis, Data curation. **Subhaswaraj Pattnaik:** Writing – review & editing, Writing – original draft, Visualization, Validation, Project administration, Methodology, Investigation, Funding acquisition, Formal analysis, Data curation. **Monika Mishra:** Writing – review & editing, Writing – original draft, Visualization, Validation, Methodology, Investigation, Formal analysis, Data curation. **Pratyush Pragyandipta:** Writing – review & editing, Visualization, Software, Resources, Methodology, Investigation, Data curation. **Animesh Pattnaik:** Writing – review & editing, Visualization, Software, Resources, Methodology, Investigation, Data curation. **Pradeep Kumar Naik:** Writing – review & editing, Writing – original draft, Validation, Supervision, Software, Resources, Project administration, Investigation, Funding acquisition, Conceptualization.

Data availability

Data will be made available on request.

Acknowledgement

The authors would like to acknowledge the Department of Biotechnology, Govt. of India (File No. BT/INF/22/SP45357/2022I) for providing financial support under DBT BUILDER. Subhaswaraj Pattnaik also likes to acknowledge the Science and Engineering Research Board (SERB), Department of Science and Technology, Govt. of India for National Post-Doctoral Fellowship (NPDF) (Ref. No. PDF/2021/001260).

Appendix A. Supplementary data

Supplementary data to this article can be found online at https://doi.org/10.1016/j.micpath.2023.106093.

References

[1] M. Jamal, W. Ahmad, S. Andleeb, F. Jalil, M. Imran, M.A. Nawaz, T. Hussain, M. Ali, M. Rafiq, M.A. Kamil, Bacterial biofilm and associated infections, J. Chin. Med. Assoc. 81 (2018) 7–11, https://doi.org/10.1016/j.jcma.2017.07.012.
[2] R. Srinivasan, S. Santhakumari, P. Poonguzhali, M. Geetha, M. Dyavaiah, L. Xiangmin, Bacterial biofilm inhibition: a focused review on recent therapeutic strategies for combating the biofilm mediated infections, Front. Microbiol. 12 (2021), 676458, https://doi.org/10.3389/fmicb.2021.676458.
[3] H. Wu, C. Moser, H.Z. Wang, N. Høiby, Z.J. Song, Strategies for combating bacterial biofilm infections, Int. J. Oral Sci. 7 (2015) 1–7, https://doi.org/10.1038/ijos.2014.65.
[4] P.M. Diaz, Impact of biofilm infection and its treatment, DJ Int. J. Adv. Microbiol. Microbiol. Res. 1 (1) (2016) 7–13, https://doi.org/10.18831/djmicro.org/2016011002.
[5] Z. Li, J. Xie, J. Yang, S. Liu, Z. Ding, J. Hao, Y. Ding, Z. Zeng, Liu, Pathogenic characteristics and risk factors for ESKAPE pathogens infection in burn patients, Infect. Drug Resist. 14 (2021) 4727, https://doi.org/10.2147/IDR.S338627.
[6] N. Vaou, E. Stavropoulou, C. Voidarou, C. Tsigalou, E. Bezirtzoglou, Towards Advances in Medicinal Plant Antimicrobial Activity: a review study on challenges and future perspectives, Microorganisms 9 (10) (2021) 2041, https://doi.org/10.3390/microorganisms9102041.
[7] M. Simoes, R.N. Bennett, E.A. Rosa, Understanding antimicrobial activities of phytochemicals against multidrug resistant bacteria and biofilms, Nat. Prod. Rep. 26 (2017) 746–757, https://doi.org/10.1039/b821648g.

[8] A. Unlu, T. Sar, G. Seker, A.G. Erman, E. Kalpar, M.Y. Akbas, Biofilm formation by *Staphylococcus aureus* strains and their control by selected phytochemicals, Int. J. Dairy Technol. 71 (2018) 637–646, https://doi.org/10.1111/1471-0307.12520.
[9] W.A. Nogueira Jose, R.A. Costa, M.T. da Cunha, T.T. Cavalcante, Antibiofilm activity of natural substances derived from plants, Afr. J. Microbiol. Res. 11 (26) (2017) 1051–1060, https://doi.org/10.5897/AJMR2016.8180.
[10] E. Sánchez, C.R. Morales, S. Castillo, C. Leos-Rivas, L. García-Becerra, D. M. Martínez, Antibacterial and antibiofilm activity of methanolic plant extracts against nosocomial microorganisms, 2016, Evid. base Compl. Alternative Med. (2016), 1572697, https://doi.org/10.1155/2016/1572697.
[11] N. Gomez-Sequeda, M. Caceres, E.E. Stashenko, W. Hidalgo, Antimicrobial and antibiofilm activities of essential oils against *Escherichia coli* O157:H7 and Methicillin-resistant *Staphylococcus aureus* (MRSA), Antibiotics 9 (2020) 730, https://doi.org/10.3390/antibiotics9110730.
[12] D. Gheorghita, A. Robu, A. Antoniac, L.M. Ditu, A.D. Raiciu, J. Tomescu, E. Grosu, A. Saceleanu, In vitro antibacterial activity of some plant essential oils against four different microbial strains, Appl. Sci. 12 (2022) 9482, https://doi.org/10.3390/app12199482.
[13] N. Nasim, J.K. Behera, I.S. Sandeep, V.V. RamaRao, B. Kar, A. Mishra, S. Nayak, S. Mohanty, Phytochemical analysis of flower from *Pandanus odorifer* (Forssk.) Kuntze for industrial application, Nat. Prod. Res. 32 (20) (2018) 1–4, https://doi.org/10.1080/14786419.2017.1422184.
[14] P. Cheruvanachari, S. Pattnaik, M. Mishra, P. Pragyandipta, P.K. Naik, Terpinen-4-ol, an active constituent of kewda essential oil, mitigates biofilm forming ability of multidrug resistant *Staphylococcus aureus* and *Klebsiella pneumoniae*, J. Biol. Active Prod. Nat. 12 (5) (2022) 406–420, https://doi.org/10.1080/22311866.2022.2154264.
[15] A. Das, S. Dey, R.K. Sahoo, S. Sahoo, E. Subudhi, Antibiofilm and antibacterial activity of essential oil bearing *Zingiber officinale* Rosc. (Ginger) Rhizome against multi-drug resistant isolates, J. Essential. Oil Bearing. Plants. 22 (2019) 1163–1171, https://doi.org/10.1080/0972060X.2019.1683080.
[16] A. Al Saqr, M.F. Aldawsari, E.S. Khafagy, M.A. Shaldam, W.A.H. Hegazy, H. A. Abbas, A novel use of allopurinol as a quorum-sensing inhibitor in *Pseudomonas aeruginosa*, Antibiotics 10 (2021) 1385, https://doi.org/10.3390/antibiotics10111385.
[17] M.D.O. Negreiros, Â. Pawlowski, C.A. Zini, G.L.G. Soares, A.D.S. Motta, A.P. G. Frazzon, Antimicrobial and antibiofilm activity of *Baccharis psiadioides* essential oil against antibiotic-resistant *Enterococcus faecalis* strains, Pharmaceut. Biol. 54 (2016) 3272–3279, https://doi.org/10.1080/13880209.2016.1223700.
[18] A. Merghni, H. Marzouki, H. Hentati, M. Aouni, M. Mastouri, Antibacterial and antibiofilm activities of *Laurus nobilis* L. essential oil against *Staphylococcus aureus* strains associated with oral infections, Curr. Res. Translational. Med. 64 (2016) 29–34, https://doi.org/10.1016/j.patbio.2015.10.003.
[19] Z. Gao, W. Zhong, K. Chen, P. Tang, J. Guo, Chemical composition and anti-biofilm activity of essential oil from *Citrus medica* L. var. sarcodactylis Swingle against *Listeria monocytogenes*, Ind. Crop. Prod. 144 (2020), 112036, https://doi.org/10.1016/j.indcrop.2019.112036.
[20] I.A.S.V. Packiavathy, S. Priya, S.K. Pandian, A.V. Ravi, Inhibition of biofilm development of uropathogens by curcumin-An anti-quorum sensing agent from *Curcuma longa*, Food Chem. 148 (2014) 453–460, https://doi.org/10.1016/j.foodchem.2012.08.002.
[21] S. Wu, G. Liu, W. Jin, P. Xiu, C. Sun, Antibiofilm and anti-infective of a marine bacterial polysachharide against *Pseudomonas aeruginosa*, Front. Microbiol. 7 (2016) 102, https://doi.org/10.3389/fmicb.2016.00102.
[22] G. Radha, P.K. Naik, M. Lopus, *In vitro* characterization and molecular dynamic simulation of shikonin as a tubulin-targeted anticancer agent, Comput. Biol. Med. 147 (2022), 105789, https://doi.org/10.1016/j.compbiomed.2022.105789.
[23] S. Santoshi, P.K. Naik, Molecular insight of isotypes specific β-tubulin interaction of tubulin heterodimer with noscapinoids, J. Comput. Aided Mol. Des. 28 (2014) 751–763, https://doi.org/10.1007/s10822-014-9756-9.
[24] R.A. Friesner, J.L. Banks, R.B. Murphy, T.A. Halgren, J.J. Klicic, D.T. Mainz, M. P. Repasky, E.H. Knoll, M. Shelley, J.K. Perry, D.E. Shaw, P. Francis, P.S. Shenkin, Glide: a new approach for rapid, accurate docking and scoring. 1. Method and assessment of docking accuracy, J. Med. Chem. 47 (7) (2004) 1739–1749, https://doi.org/10.1021/jm0306430.
[25] T.A. Halgren, R.B. Murphy, R.A. Friesner, H.S. Beard, L.L. Frye, W.T. Pollard, J. L. Banks, Glide: a new approach for rapid, accurate docking and scoring. 2. Enrichment factors in database screening, J. Med. Chem. 47 (7) (2004) 1750–1759, https://doi.org/10.1021/jm030644s.
[26] M. Martin, Cutadapt removes adapter sequences from high-throughput sequencing reads, EMBnet J 17 (1) (2011) 10–12, https://doi.org/10.14806/ej.17.1.200.
[27] C. Trapnell, A. Roberts, L. Goff, G. Pertea, D. Kim, D.R. Kelley, H. Pimentel, S. L. Salzberg, J.L. Rinn, L. Pachter, Differential gene and transcript expression analysis of RNA-seq experiments with TopHat and Cufflinks, Nat. Protoc. 7 (2012) 562–578, https://doi.org/10.1038/nprot.2012.016.
[28] D. Kim, B. Langmead, S.L. Salzberg, HISAT: a fast spliced aligner with low memory requirements, Nat. Methods 12 (4) (2015) 357–360, https://doi.org/10.1038/nmeth.3317.
[29] L.O. Felix, B. Mishra, R. Khader, N. Ganesan, E. Mylonakis, *In vitro* and *in vivo* bactericidal and antibiofilm efficacy of Alpha Mangostin against *Staphylococcus aureus* persister cells, Front. Cell. Infect. Microbiol. 12 (2022), 898794, https://doi.org/10.3389/fcimb.2022.898794.
[30] Y. Chen, T. Liu, K. Wang, C. Hou, S. Cai, Y. Huang, Z. Du, H. Huang, J. Kong, Y. Chen, Baicalein inhibits *Staphylococcus aureus* biofilm formation and the quorum sensing system *in vitro*, PLoS One 11 (4) (2016), e0153468, https://doi.org/10.1371/journal.pone.0153468.
[31] Y. Ding, Y. Onodera, J.C. Lee, D.C. Hooper, NorB, an efflux pump in *Staphylococcus aureus* strain MW2, contributes to bacteria fitness in abscesses, J. Bacteriol. 190 (21) (2008) 7123–7129, https://doi.org/10.1128/JB.00655-08.
[32] J. Tang, M. Kang, H. Chen, Y. Zheng, S. Tang, X.D. Zi, R. Zhang, R. Zhou, X. Shi, The influence of sae locus knockout on exoproteins in *Staphylococcus aureus*, J. Food Saf. 30 (2010) 711–720, https://doi.org/10.1111/j.1745-4565.2010/00235.x.
[33] J. Cui, H. Zhang, Z. Mo, M. Yu, Z. Liang, Cell wall thickness and the molecular mechanism of heterogenous vancomycin-intermediate *Staphylococcus aureus*, Lett. Appl. Microbiol. 72 (2021) 604–609, https://doi.org/10.1111/lam.13456.
[34] N.M. Zin, M.M. Al-shaibani, J. Jalil, A. Sukri, A.R. Al-Maleki, N.M. Sidik, Profiling of gene expression in methicillin-resistant *Staphylococcus aureus* in response to *cyclo*-(l-Val-l-Pro) and chloramphenicol isolated from *Streptomyces* sp., SUK 25 reveals gene downregulation in multiple biological targets, Arch. Microbiol. 202 (2020) 2083–2092, https://doi.org/10.1007/s00203-020-01896-x.
[35] L. Jirovetz, G. Buchbauer, E. Schmidt, Z. Denkova, A. Slavchev, A. Stoyanova, M. Geissler, Purity, antimicrobial activities and olfactory evaluations of 2-Phenylethanol and some derivatives, J. Essent. Oil Res. 20 (1) (2008) 82–85, https://doi.org/10.1080/10412905.2008.9699429.
[36] W.L. Kong, L. Rui, H. Ni, X.Q. Wu, Antifungal effect of volatile organic compounds produced by *Rahnella aquatilis* JZ-GX1 against *Colletotrichum gloeosporioides* in *Liriodendron* Chinese × *tulipifera*, Front. Microbiol. 11 (2020) 1114, https://doi.org/10.3389/fmicb.2020.01114.
[37] J.M. Morrison, K.L. Anderson, K.E. Beenken, M.S. Smeltzer, P.M. Dunman, The Staphylococcal accessory regulator, SarA, is an RNA-binding protein that modulates the mRNA turnover properties of late-exponential and stationary phase *Staphylococcus aureus* cells, Front. Cell. Infect. Microbiol. 2 (2012) 26, https://doi.org/10.3389/fcimb.2012.00026.
[38] A. Selvaraj, A. Valliammai, P. Muthuramalingam, A. Priya, M. Suba, M. Ramesh, S. K. Pandian, Carvacrol targets SarA and CrtM of Methicillin-resistant *Staphylococcus aureus* to mitigate biofilm formation and Staphyloxanthin synthesis: an *in vitro* and *in vivo* approach, ACS Omega 5 (2020) 31100–31114, https://doi.org/10.1021/acsomega.0c04252.
[39] P.S. Ganesh, K. Veena, R. Senthil, K. Iswamy, E.M. Ponmalar, V. Mariappan, A.S. S. Girija, J. Vadivelu, S. Nagarajan, D. Challabathula, E.M. Shankar, Biofilm-associated Agr and Sar quorum sensing systems of *Staphylococcus aureus* are inhibited by 3-Hydroxybenzoic acid derived from *Illicium verum*, ACS Omega 7 (2022) 14653–14665, https://doi.org/10.1021/acsomega.1c07178.
[40] C. Jenul, A.R. Horswill, Regulation of *Staphylococcus aureus* virulence, Microbiol. Spectr. 6 (1) (2018), https://doi.org/10.1128/microbiolspec.GPP3-0031-2018. GPP3-0031-2018.
[41] S.A.A. Ghafar, N.S. Salehuddin, N.Z.A. Rahman, N. Halib, R.M. Hanafiah, Transcriptomic profile analysis of *Streptococcus mutans* response to *Acmella paniculata* flower extracts, Evid. Based Compl. Alt. Med. (2022), 7767940, https://doi.org/10.1155/2022/7767940, 2022.
[42] Y. Yang, Y. Chen, G. Zhang, J. Sun, L. Guo, M. Jiang, B. Ou, W. Zhang, H. Si, Transcriptomic analysis of *Staphylococcus aureus* under the stress condition caused by *Litsea cubeba* L. essential oil via RNA sequencing, Front. Microbiol. 11 (2020) 1693, https://doi.org/10.3389/fmicb.2020.01693.
[43] N. Qin, X. Tan, Y. Jiao, L. Liu, W. Zhao, S. Yang, A. Jia, RNA-Seq-based transcriptome analysis of methicillin-resistant *Staphylococcus aureus* biofilm inhibition by ursolic acid and resveratrol, Sci. Rep. 4 (2014) 5467, https://doi.org/10.1038/srep05467.
[44] X. Tan, N. Qin, C. Wu, J. Sheng, R. Yang, B. Zheng, Z. Ma, L. Liu, X. Peng, A. Jia, Transcriptome analysis of the biofilm formed by methicillin-susceptible *Staphylococcus aureus*, Sci. Rep. 5 (2015), 11997, https://doi.org/10.1038/srep11997.
[45] X. Ao, J. Zhao, J. Yan, S. Liu, K. Zhao, Comparative transcriptomic analysis of *Lactiplantibacillus plantarum* RS66CD biofilm in high-salt conditions and planktonic cells, PeerJ 8 (2020) e9639, https://doi.org/10.7717/peerj.9639.